

# Integrated Biophysical Characterization of Tocilizumab and a Biosimilar Candidate: A Multi-Dimensional Study of Binding Kinetics, Thermal Stability, and Higher Order Structure

## Overview

The development of biosimilar monoclonal antibodies requires rigorous demonstration of structural and functional equivalence to the reference product under a regulatory "totality of evidence" framework. In this study, we present an integrated, multi-dimensional biophysical characterization of Tocilizumab, a humanized IgG1 monoclonal antibody targeting the interleukin-6 receptor (IL-6R), and a biosimilar candidate. Higher order structure (HOS), thermal stability, and binding kinetics were systematically evaluated using a complementary suite of orthogonal techniques: Digital Surface Plasmon Resonance (Digital SPR™), differential scanning fluorimetry (SUPR-DSF™), and circular dichroism (CD) spectroscopy (Chirascan™ V100).

## Introduction

The rapid expansion of the biopharmaceutical market has ushered in a new era of precision medicine, with monoclonal antibodies (mAbs) serving as the cornerstone of targeted therapy for autoimmune diseases and oncology.<sup>1</sup> The primary challenge of developing antibody drugs is understanding and characterizing their structural complexity. Unlike small molecule drugs, whose pharmacokinetic properties are governed by their chemical identity alone, the efficacy and immunogenicity of biologics depend on additional, external factors that may affect their highly dynamic structure, including the manufacturing process itself.<sup>2</sup> For example, minor variations in cell line expression, culture conditions, or purification steps can induce subtle alterations in Higher Order Structures (HOS), post-translational modifications (PTMs), charge heterogeneity or conformational stability.<sup>3-5</sup> Consequently, regulatory agencies such as the FDA and EMA mandate a "totality of evidence" approach, requiring a comprehensive structural and functional comparison between a biosimilar and the reference product.<sup>6,7</sup>

This application note will focus on Tocilizumab (Actemra®/RoActemra®), a humanized IgG1 monoclonal antibody targeting the interleukin-6 receptor (IL-6R). Tocilizumab represents a critical therapeutic intervention for rheumatoid arthritis (RA), systemic juvenile idiopathic arthritis (sJIA), and cytokine release syndrome (CRS).<sup>8-10</sup> Patent exclusivity for Tocilizumab expired in major markets around 2017, opening up a route to biosimilar development.<sup>11</sup>

## Integrated Solution for Kinetic, Stability & Structural Analysis

This application note presents a comprehensive workflow for the comparative characterization of Tocilizumab and a biosimilar candidate. By leveraging a joint instrumentation suite comprising the **Digital SPR™** platform for Surface Plasmon Resonance (SPR), the **SUPR-DSF™** for Differential Scanning Fluorimetry (DSF), and the **Chirascan™ V100** for Circular Dichroism (CD) spectroscopy, we establish a rigorous framework for assessing binding kinetics, thermodynamic stability, and structural integrity. This study demonstrates how orthogonal biophysical techniques can be integrated to provide a detailed and robust profile of biotherapeutic similarity, ultimately de-risking development and accelerating time-to-market.

## Digital Surface Plasmon Resonance: DMF-Powered Binding Kinetics

Nicoya's **Digital SPR** is the world's first fully automated benchtop digital SPR instrument. It leverages digital microfluidics (DMF) combined with nanotechnology-based sensors to precisely manipulate 350 nL sample droplets, enabling highly controlled and efficient experiments. By eliminating traditional fluidic components such as pumps and tubing, the system relies instead on disposable cartridges, simplifying operation and removing the need for cleaning or maintenance of fluidics. The Digital SPR platform delivers high-quality, real-time binding kinetics and enables rapid screening of antibody candidates against target antigens.

Since only 2  $\mu\text{L}$  of sample is required for kinetic analysis, Digital SPR is ideal in early discovery stages when material is limited. It provides detailed binding kinetics, allowing scientists to select high-affinity leads, differentiate candidates with similar  $K_D$  but different on- and off-rates, and optimize therapeutics for potency and duration of action.

### SUPR-DSF: Next-Generation Thermal Stability Screening

**SUPR-DSF** (Differential Scanning Fluorimetry) profiles protein conformational stability using intrinsic fluorescence. During a thermal ramp, protein unfolding exposes buried hydrophobic residues (tryptophan and tyrosine), causing wavelength shifts and intensity changes in the fluorescence emission spectrum. Unlike traditional DSF methods that rely on extrinsic dyes (e.g., SYPRO Orange), which may perturb protein stability or interact non-specifically with excipients, SUPR-DSF measures unfolding thermodynamics in the native state, including at formulation-relevant concentrations, without added dyes. The system supports high-throughput analysis in standard 384-well plates, determining melting temperature ( $T_m$ ) and onset temperature ( $T_{\text{onset}}$ ) for multiple domains simultaneously. SUPR-DSF can resolve independent unfolding of multiple domains, even when overlapping, providing a detailed conformational stability profile. Because biosimilars must demonstrate structural and functional similarity to the reference biologic, DSF is a key tool for comparing thermal stability between the biosimilar and reference product.

### Chirascan: The Gold Standard for HOS Analysis

Circular Dichroism (CD) spectroscopy is a well-established biophysical technique for the structural characterization of biotherapeutics. The **Chirascan** platform offers state-of-the-art CD instrumentation that enables quantitative Higher Order Structure (HOS) comparisons to assess structural similarity. Only Chirascan V100 and Chirascan Q100 systems employ a solid state, Large Area Avalanche Photodiode (LAAPD) detector that offers the high sensitivity superior to conventional photomultiplier tube (PMT) detectors that is required to discern the minor spectral differences and, in turn, structural differences that may occur between an originator and its biosimilar. The Chirascan V100 used in this study is a state of the art manual CD system, while the Chirascan Q100 offers an automated alternative equipped with liquid-handling robotics to ensure maximum efficiency and reproducibility.

## Results & Discussion

### Functional Binding Kinetics (Digital SPR)

In this study, Digital SPR was used to compare the binding kinetics of Tocilizumab and its biosimilar against IL-6R using an Fc capture assay. The capture of ligands on the human/rabbit Fc-specific surface was optimized to obtain a low ligand density while allowing for detection of all analyte concentrations sampled. Figures 1a & 1b show examples of raw data for ligand capture, association, and dissociation of analytes, and regeneration of the sensor surface for each antibody. Full surface regeneration was achieved using Gly-HCl pH 1.5.

The kinetic parameters calculated for Tocilizumab and its biosimilar binding to IL-6R are summarized in Table 1. All kinetic values were calculated using a standard 1:1 Langmuir fit, representative examples of which are displayed in Figures 2a & 2b. The derived affinity ( $K_D$ ) for both molecules was in the low nM range, 6.25 nM for Tocilizumab and 7.27 nM for the biosimilar. The binding kinetics of Tocilizumab compared closely to two previous studies where the  $K_D$  was determined to be 2.54 nM by Scatchard analysis and 9.9 nM by traditional SPR.<sup>12,13</sup> The tight binding of Tocilizumab and the biosimilar was driven by a relatively fast association rate and a slow dissociation rate, which is characteristic of high-potency therapeutic antibodies. The biosimilar's kinetic profile was statistically indistinguishable from that of the Tocilizumab reference, with  $K_D$  values falling well within the standard acceptance criteria (typically 80-125%) for bioequivalence. This confirms that the biosimilar effectively mimics the ligand-binding function of Tocilizumab, preserving the mechanism of action required to block IL-6 signaling.

**Table 1.** Kinetic parameters measured for IL-6R binding to Tocilizumab and its biosimilar

Sample	$k_a$ ( $\text{M}^{-1}\text{s}^{-1}$ )	$k_d$ ( $\text{s}^{-1}$ )	$K_D$ (nM)
Tocilizumab	$5.21 \times 10^4 \pm 1.48 \times 10^4$	$3.03 \times 10^{-4} \pm 1.05 \times 10^{-4}$	$6.25 \pm 2.70$
Biosimilar	$4.88 \times 10^4 \pm 1.52 \times 10^4$	$3.28 \times 10^{-4} \pm 5.72 \times 10^{-3}$	$7.27 \pm 2.34$



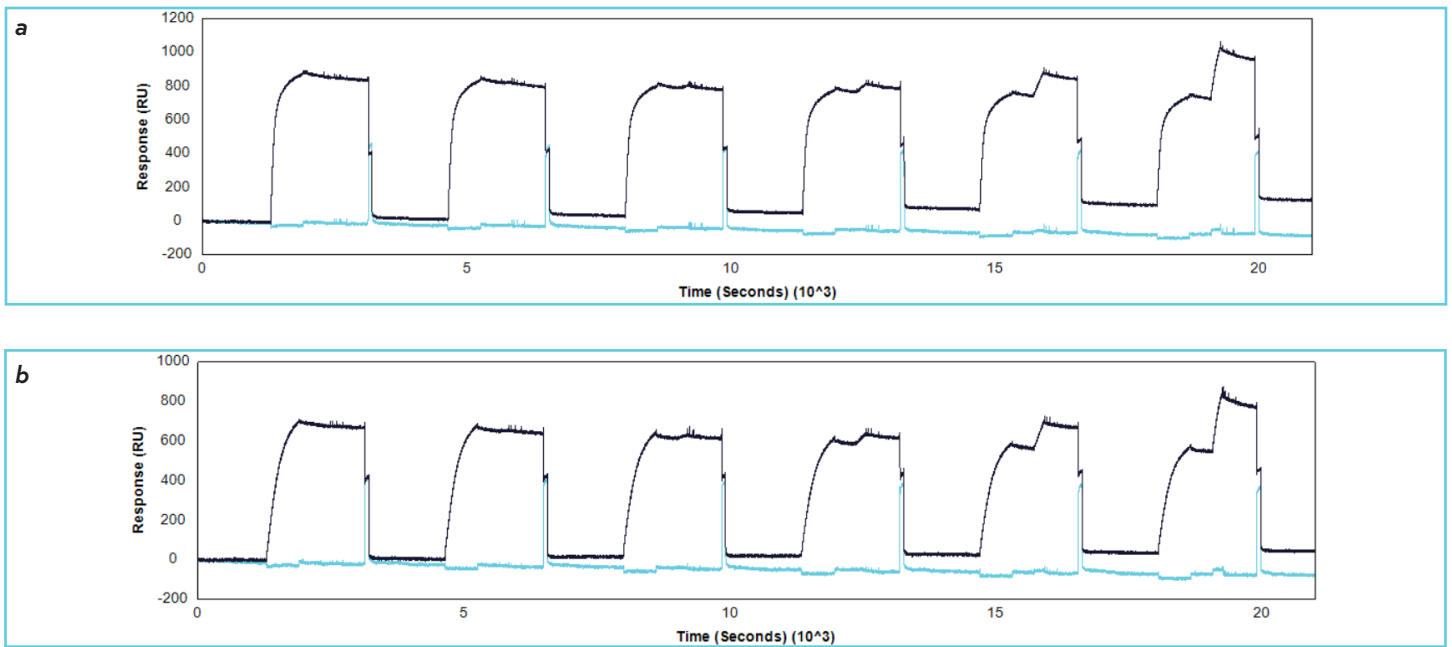


**Figure 1.** Ligand capture, IL-6R binding and regeneration for (a) Tocilizumab and (b) biosimilar. Biotinylated human Fc-specific VHH was immobilized on Nicoya Streptavidin Sensors, followed by a buffer blank where the ligand was captured on the sensor surface and running buffer was flowed over the antibody. For each cycle, 5  $\mu\text{g}/\text{mL}$  of ligand was captured on the anti-Fc surface followed by association and dissociation of the analyte, IL-6R, and regeneration. Active channel response is shown in black and the reference channel response is shown in light blue.

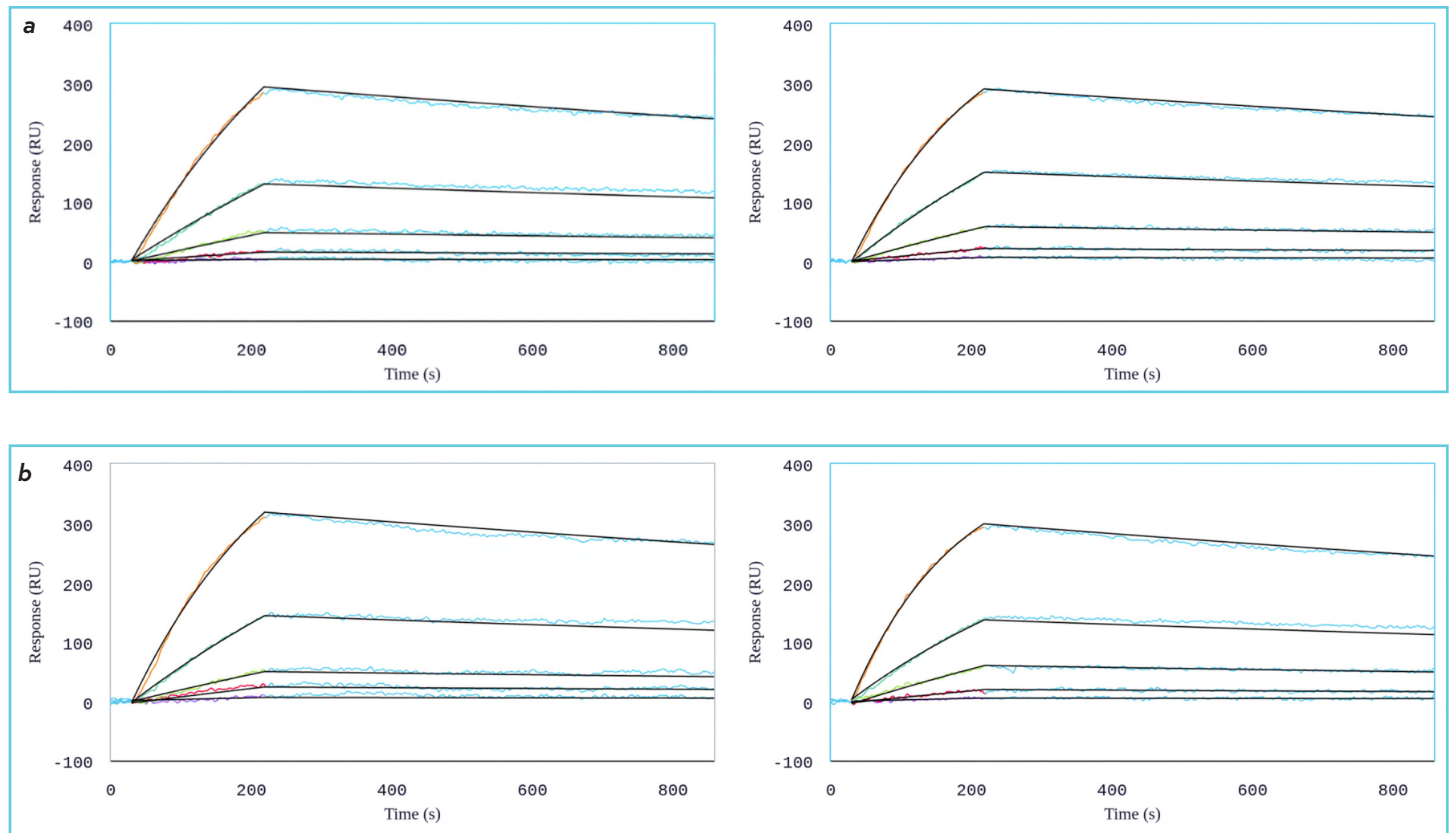


**Figure 2.** Representative kinetic fits in duplicate for IL-6R binding to (a) Tocilizumab and (b) biosimilar captured on Nicoya's human Fc-specific capture kit using multi-cycle kinetics (MCK). Kinetic fits are shown in duplicate to highlight data reproducibility. The analyte concentrations of the five curves from low to high were 1.23 nM, 3.7 nM, 11.1 nM, 33 nM and 100 nM, with the association phase of each curve indicated in orange. The dissociation phase is indicated in light blue and the Langmuir 1:1 binding fit is shown in black.

## Thermal Stability Profiling (SUPR-DSF)

Thermal unfolding is a sensitive probe of domain-level stability and can reveal subtle differences in higher-order structure arising from charge heterogeneity, glycosylation, or other post-translational modifications (PTMs) that may not be apparent from room-temperature measurements alone. Biosimilars must demonstrate high similarity to the reference biologic in structure, function, and stability, and DSF enables direct comparison of thermal stability profiles between the biosimilar and reference product. Similar  $T_m$  values suggest similar structural susceptibility to environmental conditions that promote degradation.

IgG subclass antibodies are multidomain proteins that typically unfold through multiple, sometimes partially overlapping thermal transitions, reflecting the distinct stabilities of the Fab and Fc domains. Under mild thermal stress, even at temperatures below the first domain denaturation temperature, transient unfolding of a single domain can be sufficient to initiate aggregation, with the CH2 domain frequently acting as the most thermally labile region and a key trigger for instability.<sup>14</sup> Because antibody aggregates can negatively impact therapeutic efficacy and patient safety (e.g., via increased immunogenicity risk), assessing and understanding protein unfolding and aggregation propensity is a critical part of developability and biosimilar comparability assessments. Importantly, while CH2 is often the least stable Fc domain, the location of the Fab transition can vary widely across therapeutic IgGs (and can vary widely depending on the variable region sequence), meaning that the unfolding order is not always fixed across all antibodies.<sup>15</sup> For biosimilar developers, close agreement in the number, position, and relative spacing of these thermal transitions between the reference and proposed biosimilar provides orthogonal evidence of higher-order structural similarity. In many IgG1 antibodies with average Fab stability, the observed domain melting behavior is commonly consistent with CH2 unfolding first, followed by Fab, and then the high-stability CH3 domain.<sup>16</sup>

For example, DSC analysis of Tocilizumab has been reported to exhibit three well-resolved thermal transitions that are assigned to the unfolding of the CH2, Fab, and CH3 domains, respectively, supporting a clear multidomain unfolding model for this IgG1 antibody.<sup>17</sup> Consistent with this established behavior, our DSF-based thermal denaturation experiment likewise revealed a clear multidomain unfolding profile for Tocilizumab.

The SUPR-DSF spectral data were processed to calculate the Barycentric Mean (BCM) of the fluorescence emission from 310–390 nm (fluorescence signal >390 nm was very low) at each 0.5°C temperature interval.

An example of an emission spectrum for a single temperature with its calculated BCM is shown in Figure 3a. The BCM is a center-of-mass calculation that is highly sensitive to the redshift associated with tryptophan exposure to water (tryptophan peak maximum near 335 nm), as well as tyrosine residues with an emission maximum around 315 nm.

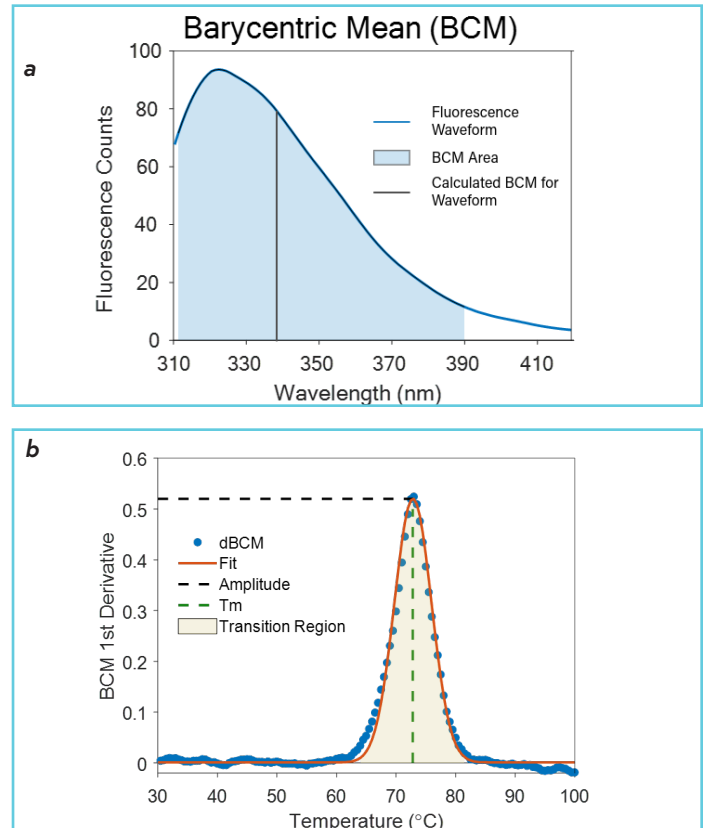


**Figure 3.** (a) The BCM method calculates wavelength shifts by measuring the center of mass of the fluorescence waveform, thereby taking advantage of the entire spectrum to increase sensitivity. 337 nm (vertical line) was calculated to be the BCM. (b) first derivative (dBCM) fitting data. The Gaussian model is effective at fitting first derivative melt curves.

A BCM plot was obtained by plotting calculated BCM values against temperature, and the first derivative of the BCM curve (Figure 3b) was calculated to identify inflection points, which correspond to the melting temperatures ( $T_m$ ) of the individual protein domains. The inflection points, now represented as positive peaks (red-shift) or negative peaks (blue-shift) were fitted with Gaussian functions to quantitatively identify the melting transitions. Onset temperatures ( $T_{onset}$ ) were determined from the point where the BCM signal first deviated (>1%) from the pre-transition baseline.



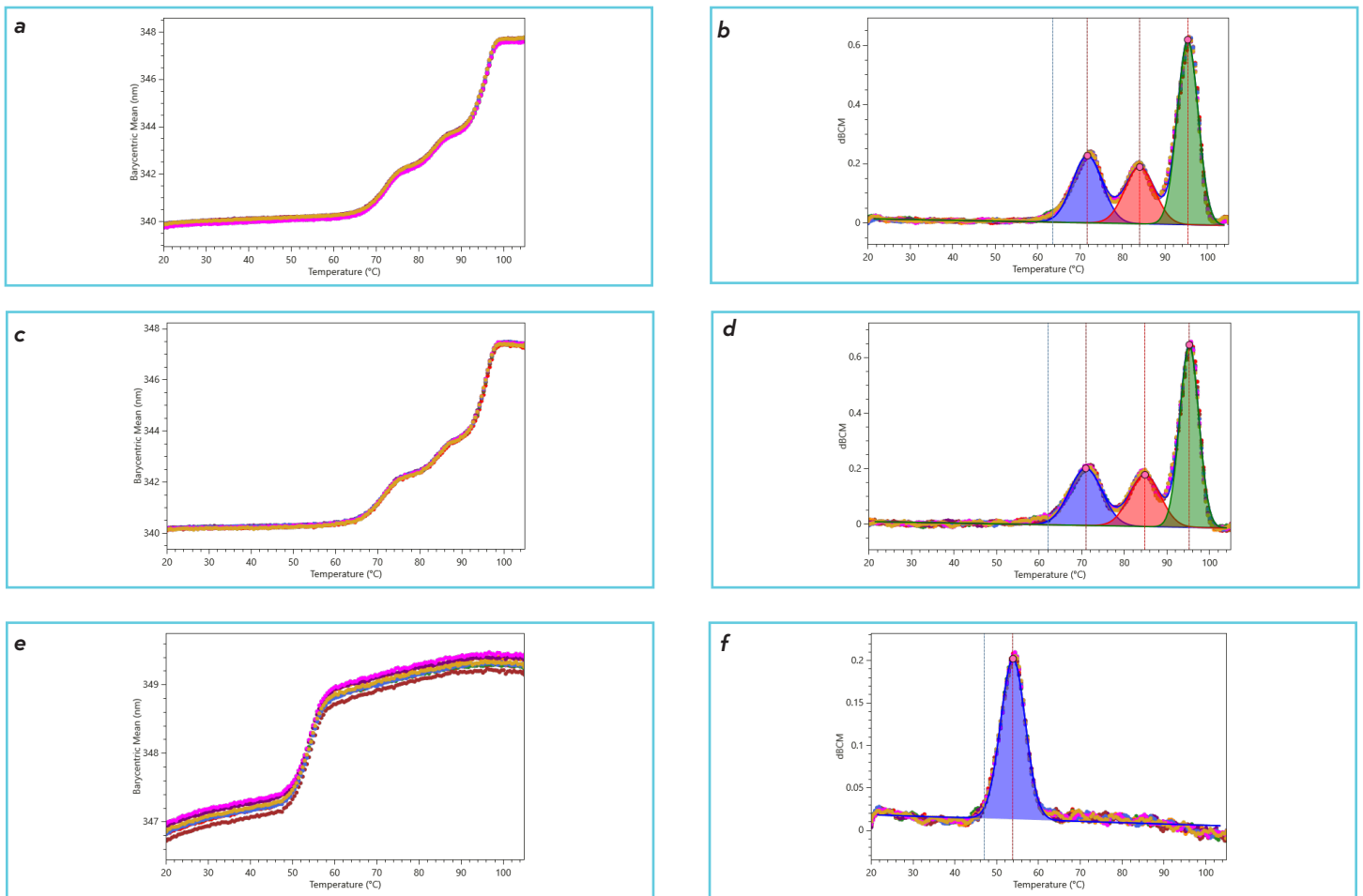


**Figure 4.** Barycentric Mean (BCM) plots for a) Tocilizumab, c) biosimilar and e) IL6, and first derivative BCM (dBCM) plots for b) Tocilizumab, d) biosimilar, f) IL6. In dBCM plots, the red line represents  $T_m$  and the blue line represents  $T_{onset}$ . The blue, red, and green shaded areas represent the temperature regions of unfolding transitions corresponding to melting temperatures  $T_{m1}$ ,  $T_{m2}$ , and  $T_{m3}$ , respectively.

## Unfolding Transitions

All samples were analyzed in eight replicates, providing high precision and strong statistical power. Applying the BCM analysis method generated high-definition melting curves from the corresponding fluorescence waveforms (Figures 4a, 4c & 4e). The resulting first-derivative traces (Figures 4b, 4d & 4f) resolved the three distinct thermal transitions previously reported for Tocilizumab.<sup>17</sup> To confirm the integrity of the antigen under the conditions used in this study, IL-6R was also subjected to DSF measurements, which showed a single unfolding transition. Gaussian peak fitting of the averaged dBCM profiles was used to determine the melting temperatures ( $T_m$ ), which are summarized below and reported in Table 2.

- **Tocilizumab Onset of Unfolding ( $T_{onset} \sim 62-63^\circ\text{C}$ ):**  $T_{onset}$  is the temperature at which the protein unfolding transition begins, defined here as the point where the intrinsic fluorescence signal (typically the BCM or 355/330 nm ratio) first deviates measurably (>1%) from its baseline as temperature increases.

- **Tocilizumab Transition 1 ( $T_{m1} \sim 71-72^\circ\text{C}$ ):** This peak likely corresponds to the unfolding of the CH2 domain in the Fc region. The CH2 domain is stabilized by N-linked glycosylation at Asn299.<sup>17</sup> A shift in  $T_{m1}$  might indicate differences in glycan structure. The biosimilar matched the reference  $T_{m1}$  within  $0.8^\circ\text{C}$ , suggesting highly similar Fc glycosylation and stability.
- **Tocilizumab Transition 2 ( $T_{m2} \sim 84-85^\circ\text{C}$ ):** This transition is attributed to the unfolding of the Fab domain. The high thermal stability of the Tocilizumab Fab reflects the rigid framework of the humanized IgG1. The biosimilar exhibited a  $T_{m2}$  value approximately  $0.8^\circ\text{C}$  higher, confirming that the antigen-binding region retains the robust conformational stability of the reference.
- **Tocilizumab Transition 3 ( $T_{m3} \sim 95^\circ\text{C}$ ):** The final transition likely corresponds to the highly stable CH3 domain. The difference in the  $T_{m3}$  value between reference and biosimilar is virtually identical at  $0.1^\circ\text{C}$ .



- **IL-6R:** The receptor exhibits a  $T_{\text{onset}}$  at  $\sim 47.0^\circ\text{C}$  and a single  $T_m$  at  $\sim 53.9^\circ\text{C}$ , consistent with a single unfolding transition and further confirming the integrity of the antigen used throughout this study.

In summary, Tocilizumab and the biosimilar exhibit the expected three distinct melting transitions, with all corresponding peaks occurring within  $<1^\circ\text{C}$  of each other (Table 2).

All standard deviation values were  $<0.2^\circ\text{C}$ , which is typical for  $T_m$  values obtained in triplicate using the SUPR-DSF. This close alignment in conformational stability supports a high degree of structural similarity between the samples and demonstrates sufficient thermal stability for a high quality biosimilar candidate. For visual comparison, an overlay of the dBCM plots for Tocilizumab and the biosimilar is shown in Figure 5.

**Table 2.**  $T_{\text{onset}}$  and  $T_m$  values measured with corresponding standard deviations.

Construct	$T_{\text{onset}}$ ( $^\circ\text{C}$ )	$T_{m1}$ ( $^\circ\text{C}$ )	$T_{m2}$ ( $^\circ\text{C}$ )	$T_{m3}$ ( $^\circ\text{C}$ )
Tocilizumab	$63.51 \pm 0.13$	$71.70 \pm 0.05$	$84.03 \pm 0.07$	$95.33 \pm 0.09$
Biosimilar	$62.02 \pm 0.18$	$70.91 \pm 0.07$	$84.82 \pm 0.11$	$95.24 \pm 0.10$
IL-6R	$46.99 \pm 0.07$	$53.89 \pm 0.02$	—	—

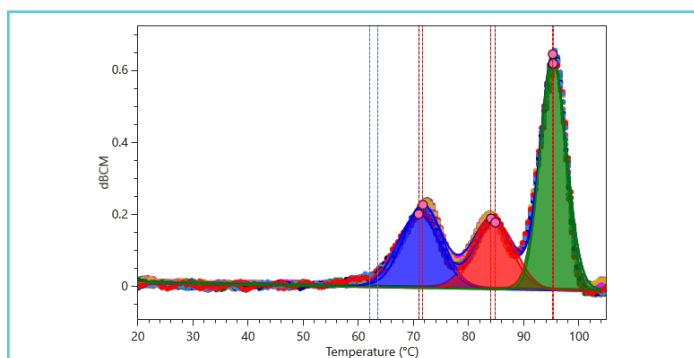


**Figure 5.** Overlay of Tocilizumab and biosimilar dBCM plots where the red line represents  $T_m$  and the blue line represents  $T_{\text{onset}}$ . The blue, red, and green shaded areas represent the temperature regions of unfolding transitions corresponding to melting temperatures  $T_{m1}$ ,  $T_{m2}$ , and  $T_{m3}$  respectively.

## Statistical Significance

A two-sample Student's t-test (unpaired, two-tailed) was conducted on the SUPR-DSF data to determine true statistical significance (Table 3). Using a threshold of  $p = 0.05$ , it can be seen that  $T_{m1}$  and  $T_{m2}$  are different, whereas  $T_{m3}$  is the same between Tocilizumab and the biosimilar.

While far-UV CD demonstrated similarity in secondary structure (see next section), SUPR-DSF measurements are fluorescence-based and, therefore, probe tertiary structure. The slight differences in melting transition temperatures observed by DSF may be attributable to minor variations in the Fab amino acid sequence between the two samples.

**Table 3.** T-test results for each  $T_m$  of Tocilizumab.

T-Test	$T_{m1}$	$T_{m2}$	$T_{m3}$
$p = 0.05$ threshold	$3.81 \times 10^{-13}$	$8.98 \times 10^{-11}$	0.0641

## Structural Characterization and Higher Order Structure Comparison (Chirscan V100)

Far-UV CD spectra with a high signal-to-noise ratio were obtained for all proteins. The far-UV CD spectrum for IL-6R showed a particularly interesting profile as it is unlike spectra most commonly observed for proteins dominated by  $\beta$ -sheet structure (Figure 6a). A positive peak observed at 230 nm might arise from disulfide bonds, which are known to contribute in this spectral region and of which there are 4 in the IL-6R protein.

While this spectrum appears atypical,  $\beta$ -sheet proteins are known to show a larger spectral diversity than  $\alpha$ -helical proteins,<sup>18</sup> and results obtained with secondary structure decomposition analysis using BeStSel agreed well (within  $\pm 3\%$  for each secondary structure element) with the secondary structure composition as calculated from the crystal structure of the extra-cellular domains of the Human IL-6R alpha chain (Table 4).

**Table 4.** Comparison of IL-6R secondary structure analysis on far-UV CD to crystal structure.

Element	Content (%)	
	Experimental (from far-UV CD data)	Calculated (from PDB ID 1N26)
Helix (Regular)	0	0
Helix (Distorted)	0	0
Anti-parallel $\beta$ -sheet (left-twisted)	0	1
Anti-parallel $\beta$ -sheet (relaxed)	21	20
Anti-parallel $\beta$ -sheet (right-twisted)	19	17
Parallel $\beta$ -sheet	0	2
Others	46	49
Turn	14	11



Far-UV CD data were also obtained for IL-6R in the presence of Tocilizumab at a 1:1 molar ratio, but these results did not suggest that binding between the immunoglobulin and the receptor is accompanied by any significant changes in secondary structure, as the spectrum for the mixture was virtually identical to the composite spectrum obtained from averaging the spectra for the individual molecules (Figure 6b).

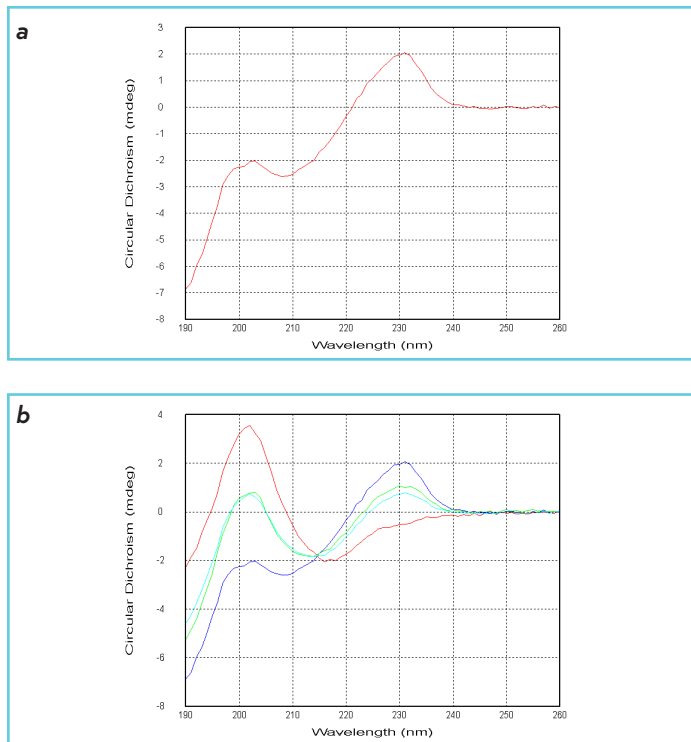


**Figure 6.** (a) Averaged and baseline-corrected far-UV CD spectrum of IL-6R, (b) Individual far-UV CD spectra of Tocilizumab (red) and IL-6R (blue), spectrum for 1:1 mixture (green), and composite spectrum (cyan).

Spectral profiles for Tocilizumab and its biosimilar were characterized by two main peaks just above 200 nm and 215 nm (Figures 7a-d), as expected: this indicates that secondary structure was dominated by  $\beta$ -sheet content as is typical for the Fab and Fc domains of immunoglobulins. Moreover, a shoulder around 230 nm can be attributed to disulfide bond contributions. Raw CD spectra showed minor variability in overall intensity amongst replicates due to manual handling and cleaning of demountable sample cells, which was accounted for by normalisation by absolute area for subsequent HOS comparison analysis.

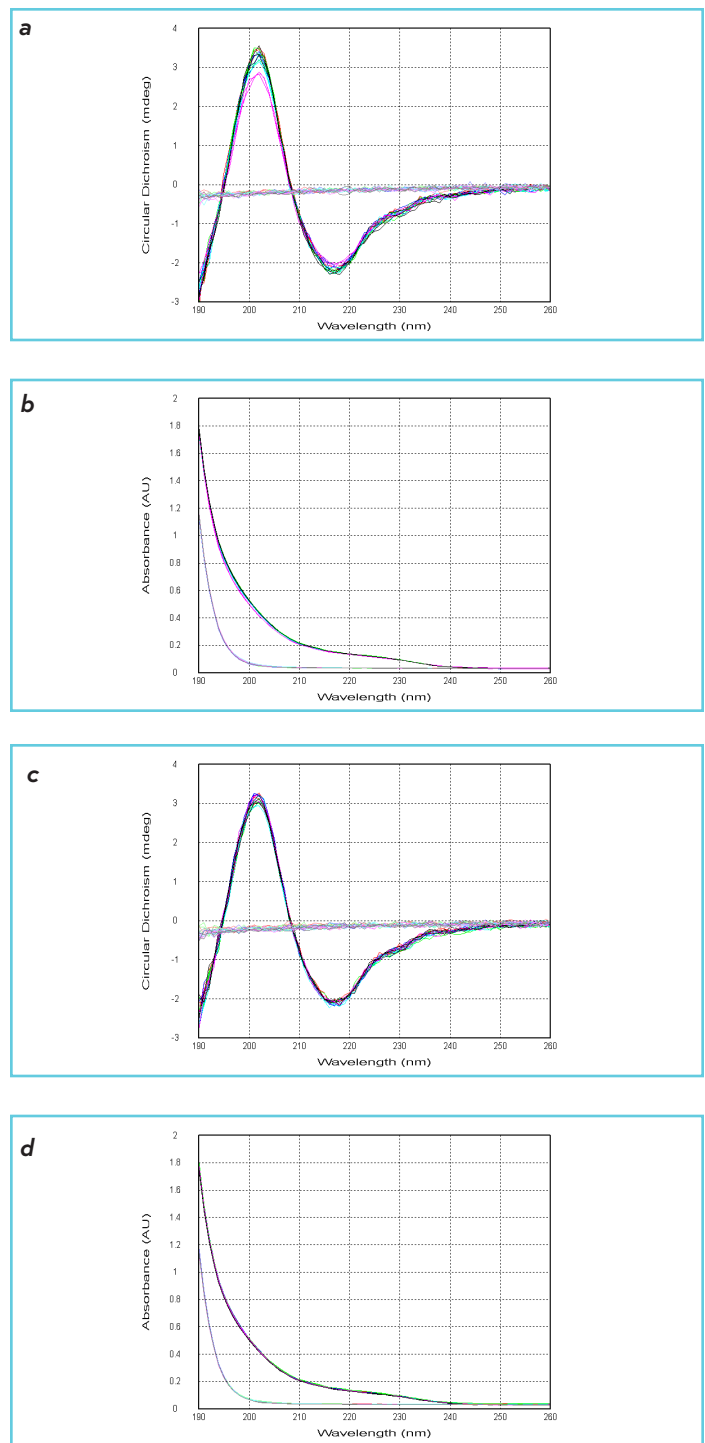


**Figure 7.** Raw far-UV CD spectra (a and c) and absorbance spectra (b and d) of Tocilizumab (a and b) and its biosimilar (c and d). Each plot shows a total of 36 traces, including 3 repeat scans for each of 6 replicate measurements for both sample and buffer blank.

In a first instance, the HOS of an originator and its biosimilar can be compared by visually evaluating the similarity of normalized CD spectra, as done previously.<sup>17</sup> Well-overlapping far-UV CD spectra for Tocilizumab and its biosimilar suggested a high similarity of secondary structure (Figure 8).



However, visual assessment alone is prone to user bias and, thus, lacks reliability. Therefore, similarity was confirmed quantitatively by means of a HOS comparison analysis via the Weighted Spectral Difference (WSD) comparability method.

In brief, this approach yields a value as a measure of similarity for the pair-wise comparison of any two spectra, where a WSD value of zero would indicate identical spectra, and larger WSD values indicate reduced similarity. To establish a quality range to test against, such pair-wise comparisons are first carried out within the set of reference replicates only. A quality range can then be defined based on the mean and standard deviation (SD) of these reference similarity values. In a second step, similarity values are obtained for comparisons between reference and sample replicates (here: Tocilizumab and biosimilar, respectively). Spectral differences observed for a sample replicate can be considered significant if the corresponding similarity value falls outside of the defined quality range.

Typically, a quality range centered at the reference mean and spanning two times the reference SD below and above the mean ( $\pm 2x$  SD) is used. To facilitate evaluation against the quality range, the WSD similarity values were evaluated in terms of Z-scores, i.e., normalized to the reference SD (Table 5). All Z-scores for reference-to-sample comparisons were  $< 2$ , demonstrating that similarity values for all sample replicates fell within the chosen quality range, and, in turn, suggesting the absence of any significant spectral differences. Statistical analysis with a Student's t-test yielded a p-value of 0.162, confirming that spectral differences in the far-UV, and therefore differences in secondary structure, cannot be considered statistically significant based on a threshold of  $p = 0.05$ .

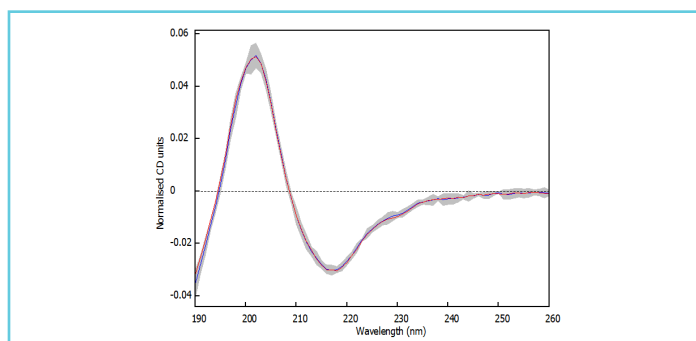


**Figure 8.** Tocilizumab (blue) and biosimilar (red) far-UV CD spectra after averaging of repeat scans, baseline correction, normalization by absolute area, and averaging of all replicates, together with  $2x$  SD reference error band (gray).

**Table 5.** Z-Scores for weighted spectral difference.

Replicate	Tocilizumab (Reference)	Biosimilar (Sample)
1	0.684	0.441
2	-0.168	0.0989
3	-0.873	1.38
4	0.138	0.153
5	1.47	1.07
6	-1.25	1.25

## Discussion

The integrated biophysical characterization of Tocilizumab and its biosimilar candidate demonstrates a high degree of similarity across structure, stability, and function, consistent with regulatory expectations for biosimilar approval. Digital SPR analysis confirmed that both Tocilizumab and the biosimilar bind IL-6R with high affinity and comparable kinetics. The derived  $K_D$  values (6.25 nM vs. 7.27 nM) fall well within established bioequivalence acceptance criteria, indicating that the biosimilar maintains the receptor-blocking mechanism of the originator. The observed association and dissociation rates further support functional equivalence, demonstrating that the biosimilar maintains the slow dissociation characteristic of high-potency therapeutic antibodies.

Thermal stability profiling via SUPR-DSF provided complementary evidence of structural equivalence. The three distinct unfolding transitions observed for both Tocilizumab constructs correspond to the CH2, Fab, and CH3 domains, with  $T_m$  and  $T_{onset}$  values differing by less than  $1^\circ\text{C}$ . Statistical analysis revealed only minor differences in  $T_{m1}$  and  $T_{m2'}$ , suggesting a high degree of structural similarity between the samples. As indicated by the high similarity in binding kinetics, any subtle differences in tertiary structure did not translate into any functional discrepancies. The strong agreement between DSF and previously published DSC data reinforces the reliability of thermal stability as a proxy for protein conformational integrity and DSF results confirm that the thermal stability of the biosimilar is comparable to that of Tocilizumab, indicating a good biosimilar candidate.

Finally, CD spectroscopy established structural characterization for both antibody and antigen and, in combination with secondary structure decomposition analysis, corroborated a high  $\beta$ -sheet content for IL-6R that matches that derived from its crystal structure. More importantly, HOS comparison analysis of the far-UV CD spectra of Tocilizumab and its biosimilar revealed that spectral differences were statistically insignificant, indicating highly similar secondary structure.



Moreover, the IL-6R binding experiment demonstrated that complex formation did not perturb the receptor's secondary structure. These results confirm that the biosimilar maintains the structural integrity of the reference molecule, a critical determinant of therapeutic function and immunogenicity.

The combination of orthogonal biophysical techniques allows for a comprehensive "totality of evidence" approach. Digital SPR confirms functional ligand binding, SUPR-DSF sensitively interrogates domain thermal stability and CD spectroscopy captures secondary and tertiary structure. This triangulated strategy mitigates the risk of undetected deviations in structure, stability, or function, which is critical for monoclonal antibodies where minor variations can impact immunogenicity or therapeutic efficacy. The high reproducibility and statistical robustness of the assays enhance confidence in the biosimilarity assessment, supporting regulatory submissions and informing quality-by-design approaches in manufacturing.

## Conclusion

The rigorous characterization of biosimilars demands a holistic view of the molecule. This application note demonstrates that the **Digital SPR**, **SUPR-DSF** and **Chirascan** platforms form a versatile toolkit for this purpose.

This study confirmed that Tocilizumab and the biosimilar candidate are:

- **Functionally Equivalent:** Binding the IL-6R target with nanomolar affinity ( $K_D \sim 7$  nM) and identical kinetic rate constants.
- **Thermodynamically Equivalent:** Exhibiting matching unfolding transitions for the CH2, Fab, and CH3 domains.
- **Structurally Equivalent:** Displaying a secondary structure profile that is statistically equivalent

By utilizing this joint instrument workflow, scientists can achieve a deeper understanding of their molecules earlier in the pipeline, ensuring that only the most robust and similar candidates progress to clinical trials. This integrated approach not only satisfies the "totality of evidence" regulatory requirement but also paves the way for more efficient, safe, and cost-effective delivery of life-changing biologics to patients.

## Materials & Methods

### Biological Sample Information

The following commercially available samples were used for the experimental procedures conducted:

- Tocilizumab (Selleckchem, Cat # A2012)
- Tocilizumab Biosimilar (InvivoGen, Cat # hil6rto-mab1)
- Recombinant Human IL-6R Protein (Sino Biological, Cat # 10398-H08H)

### Digital Surface Plasmon Resonance

Binding kinetics were measured using a capture-based assay on an Alto 16-channel Digital SPR instrument with Nicosystem Pro software (DSPR16-PRO). A biotinylated human/rabbit Fc-specific VHH from the Nicoya human/rabbit VHH kit (DSPR-VHH-HR-KIT) was immobilized on a Streptavidin cartridge (KC-STV-CMD-16) and Tocilizumab and its biosimilar were captured for interrogation against IL-6R. This orientation ensures that the Tocilizumab Fc region is tethered, exposing both Fab arms for binding to the IL-6R analyte, thereby mimicking the physiological interaction.

[Nicoya's eBook: Mastering kinetic binding assays](#) walks through the assay development steps for determining the optimal experimental conditions for analyzing kinetics on Digital SPR platforms. This includes guidance on ligand loading density, analyte concentration, buffer conditions, and regeneration for obtaining accurate and reliable kinetics and affinities.

### Capture kinetics of IL-6R to Tocilizumab and its biosimilar on a Streptavidin Cartridge

Default drop timings were used unless otherwise indicated.

1. **Reconstitution:** The lyophilized proteins were reconstituted in sterile water according to the manufacturer's instructions to generate a stock solution.
2. **Normalization:** Streptavidin sensors were normalized with normalization solutions.
3. **Immobilization:** 5 µg/mL biotinylated Fc-specific VHH diluted in PBST was immobilized onto all sensors.
4. **Conditioning:** All sensors were conditioned with 10 mM Gly-HCl, pH 1.5.
5. **Automated Serial Dilution:** The Alto Digital SPR automatically executed a five-step, threefold serial dilution on the cartridge with running buffer. A 300 nM stock of IL-6R yielded 1.23 nM, 3.7 nM, 11.1 nM, 33 nM and 100 nM solutions.



- 6. Buffer Blank:** Even sensors were exposed to either 5  $\mu\text{g}/\text{mL}$  Tocilizumab or biosimilar for 300 s. All sensors were then exposed to running buffer and regenerated with 10 mM Gly HCl pH 1.5.
- 7. Kinetics:** Even sensors were exposed to either 5  $\mu\text{g}/\text{mL}$  Tocilizumab or biosimilar. All sensors were then exposed to the lowest IL-6R concentration, allowed to dissociate in running buffer, and regenerated with 10 mM Gly HCl, pH 1.5. This step was repeated for the remaining four IL-6R concentrations, which then constituted a full multi-cycle kinetics (MCK) round with a buffer blank.
- 2. Sealing:** The plate was sealed with an optically clear, pressure-activated adhesive film (qPCR Adhesive Seal; Azenta Life Sciences, 4ti-0560) to prevent sample evaporation and concentration changes during the thermal ramp.
- 3. Data Acquisition:** The SUPR-DSF instrument was configured for a continuous linear thermal ramp using the following parameters:
  - *Temperature Range:* 20°C to 105°C.
  - *Ramp Rate:* 1°C per minute.
  - *Excitation:* Samples were excited at 280 nm.
  - 174 total spectra were obtained from each sample (scan interval = 0.5°C)
  - *Integration time:* 25 ms
  - *Detection:* Full spectrum fluorescence emission (310–420 nm)

## Kinetic Analysis

All interactions were automatically double-referenced in the Nicosystem by subtracting the signal from reference channels (no Tocilizumab captured) and buffer blanks (zero analyte concentration). The resulting sensorgrams were fitted to a 1:1 Langmuir binding model to extract the association rate constant  $k_a$ , dissociation rate constant  $k_d$ , and equilibrium dissociation constant  $K_D$ .

## Differential Scanning Fluorimetry

### Sample Preparation

- 1. Reconstitution:** The lyophilized proteins were reconstituted in sterile water according to the manufacturer's instructions to generate a stock solution.
- 2. Buffer Exchange:** Samples were buffer exchanged under identical conditions over three consecutive spin-concentration cycles using Amicon Ultra Centrifugal Filters (MilliPore Sigma, UFC5030; 0.5 mL, 30 kDa MWCO) following the manufacturer's directions, and using Eppendorf Centrifuge 5417R at 4°C.
- 3. Final Formulation:** The recovered samples were weighed and PBS was added to resuspend the samples to 100  $\mu\text{L}$  total (1 mg/mL nominal concentration).

### Experimental Procedure:

All samples were analyzed at a nominal concentration of 1 mg/mL in PBS.

- 1. Plate Loading & Replicates:** All samples (10  $\mu\text{L}$  aliquots per well) were pipetted into a standard black 384-well PCR microplate (FrameStar™ 384-Well Skirted PCR Plate; Azenta Life Sciences, 4ti-0386), using eight replicate wells per condition. PBS was pipetted into eight wells to serve as a buffer control.

## Data Analysis:

SUPR-Suite software (v2.0.11.0) was used for data acquisition and analysis. Spectral data were processed using the Barycentric Mean (BCM) method over 310–390 nm, and melting temperatures ( $T_m$ ) were determined from the corresponding first-derivative BCM fits using the SUPR-Suite's proprietary autofitting algorithm.

## Circular Dichroism Spectroscopy

HOS comparisons require sample(s) and reference to be in an identical buffer matrix to eliminate structural differences arising from non-identical buffer environments. A buffer exchange protocol was therefore implemented as follows.

### Sample Preparation:

- 1. Reconstitution:** The lyophilized proteins were reconstituted in sterile water according to the manufacturer's instructions to generate a stock solution.
- 2. Filter Preparation:** Amicon Ultra Centrifugal Filters (MilliPore Sigma, UFC8030; 4 mL) with a 30 kDa (Tocilizumab and biosimilar) or 10 kDa (IL-6R) molecular weight cutoff (MWCO) were used and pre-rinsed with 4 mL of Milli-Q water.
- 3. Buffer Exchange:** An aliquot of each protein was diluted to 4 mL with 1x PBS (pH 7.4) in a separate filter unit. The samples were centrifuged at 3063 RCF (4100 rpm) for 10 min (30 kDa MWCO) or 20 min (10 kDa MWCO) using a Heraeus Megafuge 11 (Rotor T41).



4. **Cycling:** The flow-through was discarded, and the retentate was re-diluted to 4 mL with fresh PBS. This concentration/dilution cycle was repeated two times to ensure a theoretical buffer exchange efficiency of >99%.
5. **Final Formulation:** The concentrated retentates were recovered and adjusted to a nominal target concentration of 1.0 mg/mL using PBS buffer. Final actual concentrations of Tocilizumab/biosimilar were determined to be ~0.8 mg/mL using UV absorbance at 205 nm. Extinction coefficients used were based on protein amino acid sequences including a total of 16 disulfide bonds for Tocilizumab and biosimilar.<sup>19-20</sup>
6. **Incubation:** For measurements of Tocilizumab in presence of IL-6R, the antibody and antigen were mixed and incubated for 1 hour at 4°C prior to measurement.

## Experimental Setup:

Measurements were conducted on a Chirascan V100 spectrometer. Six independent replicates were prepared and measured for both the reference and biosimilar to enable statistical comparison, and an individual buffer baseline was measured for each replicate. Between measurements, the sample cell was manually cleaned using detergent (10% Decon), rinsed with Milli-Q water, wiped with acetone on a lint-free tissue, and blow-dried.

- **Cell Type:** A demountable quartz cell with a path length of 0.1 mm (sample volume: 25 µL) was used. This short pathlength was most suited for analyzing the protein solutions at the given concentration (~1 mg/mL) and minimizing spectral contribution by the highly-absorbing PBS buffer, allowing for high-quality data acquisition in the deep far-UV.
- **Acquisition Parameters:**
  - *Wavelength Range:* 180 nm to 260 nm
  - *Bandwidth:* 1.0 nm.
  - *Step Size:* 1.0 nm.
  - *Time-per-point:* 1.0 s.
  - *Temperature:* 20°C.
  - *Repeat scans:* 3

## Data Processing:

Repeat scans for each measurement were averaged to improve the signal-to-noise ratio.

Average spectra were then baseline-corrected by subtracting the average spectrum of the PBS buffer from the corresponding average sample spectrum.

## Data Analysis:

For HOS comparison analysis, data down to 190 nm were used to exclude data with a maximum absorbance >2 A.U. and spectra were normalized by absolute area to eliminate spectral differences that arise merely due to slight differences in concentration. Spectral similarity was quantified using the weighted spectral difference (WSD) method<sup>21,22</sup> and a ±2 standard deviation (SD) quality range. WSD similarity values were obtained using HOS comparison software qBiC based on eq 1 where  $y_A$  and  $y_B$  represent signals of reference and sample spectra respectively and  $n$  represents the number of data points.

$$WSD = \sqrt{\sum_{i=1}^n \left(\frac{1}{n}\right) \left(\frac{|y_{Ai}|}{|y_{A|ave.}|}\right) (y_{Ai} - y_{Bi})^2} \quad (1)$$

Both secondary structure decomposition analysis for IL-6R based on processed far-UV CD data and calculation of expected secondary structure content based on its available crystal structure (PDB ID 1N26) were carried out using BeStSel (<https://bestsel.elte.hu/>).<sup>18,23-25</sup>

The former was done with input parameters including a concentration of 19.4 µM (based on nominal concentration of 1 mg/mL and a molecular weight of 51547.52 Da as calculated from its sequence (accession number NP\_000556.1) and a number of amino acids of 468.



# References

1. Walsh, G. *Biopharmaceuticals: Biochemistry and Biotechnology*, 2nd ed.; John Wiley & Sons: Chichester, U.K., 2003.
2. Beck, A.; Wurch, T.; Bailly, C.; Corvaia, N. Strategies and Challenges for the Next Generation of Therapeutic Antibodies. *Nat. Rev. Immunol.* 2010, 10(5), 345–352. <https://doi.org/10.1038/nri2747>.
3. Jefferis, R. Recombinant Antibody Therapeutics: The Impact of Glycosylation on Mechanisms of Action. *Trends Pharmacol. Sci.* 2009, 30(7), 356–362. <https://doi.org/10.1016/j.tips.2009.04.007>.
4. Berkowitz, S. A.; Engen, J. R.; Mazzeo, J. R.; Jones, G. B. Analytical Tools for Characterizing Biopharmaceuticals and the Implications for Biosimilars. *Nat. Rev. Drug Discov.* 2012, 11(7), 527–540. <https://doi.org/10.1038/nrd3746>.
5. ICH Q5E Expert Working Group. Comparability of Biotechnological/Biological Products Subject to Changes in Their Manufacturing Process (ICH Q5E); International Council for Harmonisation: Geneva, Switzerland, 2004.
6. U.S. Food and Drug Administration. Scientific Considerations in Demonstrating Biosimilarity to a Reference Product: Guidance for Industry; FDA: Silver Spring, MD, 2015.
7. European Medicines Agency. Guideline on Similar Biological Medicinal Products; EMA: London, U.K., 2014.
8. Tanaka, T.; Narazaki, M.; Kishimoto, T. IL-6 in Inflammation, Immunity, and Disease. *Cold Spring Harb. Perspect. Biol.* 2014, 6(10), a016295. <https://doi.org/10.1101/cshperspect.a016295>.
9. Mihara, M.; Kasutani, K.; Okazaki, M.; Nakamura, A.; Kawai, S.; Sugimoto, M.; Matsumoto, Y.; Ohsugi, Y. Tocilizumab Inhibits Signal Transduction Mediated by Both mL-6R and sIL-6R, but Not by the Receptors of Other Cytokines. *Int. Immunopharmacol.* 2005, 5(12), 1731–1740. <https://doi.org/10.1016/j.intimp.2005.05.010>.
10. U.S. Food and Drug Administration. Actemra (Tocilizumab) Prescribing Information; FDA: Silver Spring, MD, 2023.
11. European Medicines Agency. RoActemra: EPAR – Product Information; EMA: Amsterdam, The Netherlands, 2017.
12. Merbl, Y.; Lopez Baltazar, J. M.; Byron, M.; Chan, S. K. C.; Ehrlich, J. J.; Yu, Q. Tocilizumab Binds to Canine IL-6 Receptor and Elicits In-Vitro Inhibitory Biological Response. *Front. Vet. Sci.* 2025, 12, 1645414. <https://doi.org/10.3389/fvets.2025.1645414>.
13. Mihara, M.; Kasutani, K.; Okazaki, M.; Nakamura, A.; Kawai, S.; Sugimoto, M.; Matsumoto, Y.; Ohsugi, Y. Tocilizumab Inhibits Signal Transduction Mediated by Both mL-6R and Soluble Interleukin-6 Receptor, but Not by the Receptors of Other Members of the IL-6 Cytokine Family. *Int. Immunopharmacol.* 2005, 5(12), 1731–1740. <https://doi.org/10.1016/j.intimp.2005.05.010>.
14. Andersen, C. B.; Manno, M.; Rischel, C.; Thórólfsson, M.; Martorana, V. Aggregation of a Multidomain Protein: A Coagulation Mechanism Governs Aggregation of a Model IgG1 Antibody under Weak Thermal Stress. *Protein Sci.* 2010, 19(2), 279–290. <https://doi.org/10.1002/pro.309>.
15. Ionescu, R. M.; Vlasak, J.; Price, C.; Kirchmeier, M. Contribution of Variable Domains to the Stability of Humanized IgG1 Monoclonal Antibodies. *J. Pharm. Sci.* 2008, 97(4), 1414–1426. <https://doi.org/10.1002/jps.21104>.
16. Garber, E.; Demarest, S. J. A Broad Range of Fab Stabilities within a Host of Therapeutic IgGs. *Biochem. Biophys. Res. Commun.* 2007, 355(3), 751–757. <https://doi.org/10.1016/j.bbrc.2007.02.042>.
17. Miao, S.; Fan, L.; Zhao, L.; Ding, D.; Liu, X.; Wang, H.; Tan, W.-S. Physicochemical and Biological Characterization of the Proposed Biosimilar Tocilizumab. *Biomed. Res. Int.* 2017, 2017, 4926168. <https://doi.org/10.1155/2017/4926168>.
18. Micsonai, A. BeStSel: From Secondary Structure Analysis to Protein Fold Prediction by Circular Dichroism Spectroscopy. In *Structural Genomics: General Applications*; Humana Press, Methods in Molecular Biology; Vol. 2141; Springer: New York, NY, 2020; pp 119–131. [https://doi.org/10.1007/978-1-0716-0892-0\\_11](https://doi.org/10.1007/978-1-0716-0892-0_11).
19. Anthis, N. J.; Clore, G. M. Sequence-Specific Determination of Protein and Peptide Concentrations by Absorbance at 205 nm. *Protein Sci.* 2013, 22(6), 851–858. <https://doi.org/10.1002/pro.2253>.
20. Kuipers, B. J. H.; Gruppen, H. Prediction of Molar Extinction Coefficients of Proteins and Peptides Using UV Absorption of the Constituent Amino Acids at 214 nm To Enable Quantitative Reverse Phase High-Performance Liquid Chromatography–Mass Spectrometry Analysis. *J. Agric. Food Chem.* 2007, 55(14), 5445–5451. <https://doi.org/10.1021/jf070337l>.
21. Dinh, N. N.; Winn, B. C.; Arthur, K. K.; Gabrielson, J. P. Quantitative Spectral Comparison by Weighted Spectral Difference for Protein Higher Order Structure Confirmation. *Anal. Biochem.* 2014, 464, 60–62. <https://doi.org/10.1016/j.ab.2014.07.011>.
22. Teska, B. M.; Li, C.; Winn, B. C.; Arthur, K. K.; Jiang, Y.; Gabrielson, J. P. Comparison of Quantitative Spectral Similarity Analysis Methods for Protein Higher-Order Structure Confirmation. *Anal. Biochem.* 2013, 434(1), 153–165. <https://doi.org/10.1016/j.ab.2012.11.018>.
23. Micsonai, A.; Wien, F.; Kernya, L.; Lee, Y. H.; Goto, Y.; Réfrégiers, M.; Kardos, J. Accurate Secondary Structure Prediction and Fold Recognition for Circular Dichroism Spectroscopy. *Proc. Natl. Acad. Sci. U. S. A.* 2015, 112(24), E3095–E3103. <https://doi.org/10.1073/pnas.1500851112>.
24. Micsonai, A.; Wien, F.; Bulyáki, É.; Kun, J.; Moussong, É.; Lee, Y. H.; Goto, Y.; Réfrégiers, M.; Kardos, J. BeStSel: a Webserver for Secondary Structure and Fold Prediction for Protein CD Spectroscopy. *Nucleic Acids Res.* 2022, 50(W1), W90–W98. <https://doi.org/10.1093/nar/gkac345>.
25. Micsonai, A.; Wien, F.; Bulyáki, É.; Kun, J.; Moussong, É.; Lee, Y. H.; Goto, Y.; Réfrégiers, M.; Kardos, J. BeStSel: a Web Server for Accurate Protein Secondary Structure Prediction and Fold Recognition from the Circular Dichroism Spectra. *Nucleic Acids Res.* 2018, 46(W1), W315–W322. <https://doi.org/10.1093/nar/gky497>.

